## REMARKS

As plasma display panels (PDP) have increased in size while being required to increase the cells to be enabled for high definition television, additional problems have been experienced. This field is highly competitive with international companies competing very strongly, and cost is a major factor.

Additionally, the expenditure of energy, both for the cost of the energy and the impact of increased heat, must also be considered. The production yield is also important in order to remain competitive in this field.

These factors must be taken into consideration in evaluating improvements that address and resolve the above issues.

Our amended Claim 1 is characterized by: a plasma display panel in which a protective layer covers a dielectric layer covering electrodes in discharge cells and faces a discharge space filled with a discharge gas, wherein the discharge gas includes Xe whose partial pressure is no less than 20%, and in the protective layer, an electron band including at least electrons having energy level of 4 eV or less below a vacuum level is formed within a forbidden band in energy bands.

[0068]   FIG. 5 shows relationships between firing voltage Vf of a discharge cell and partial pressure of one constituent gas included in discharge gas of in PDPs;

351 : Xe content(%)
352 : Xe content(%)
353 : Kr content(%)
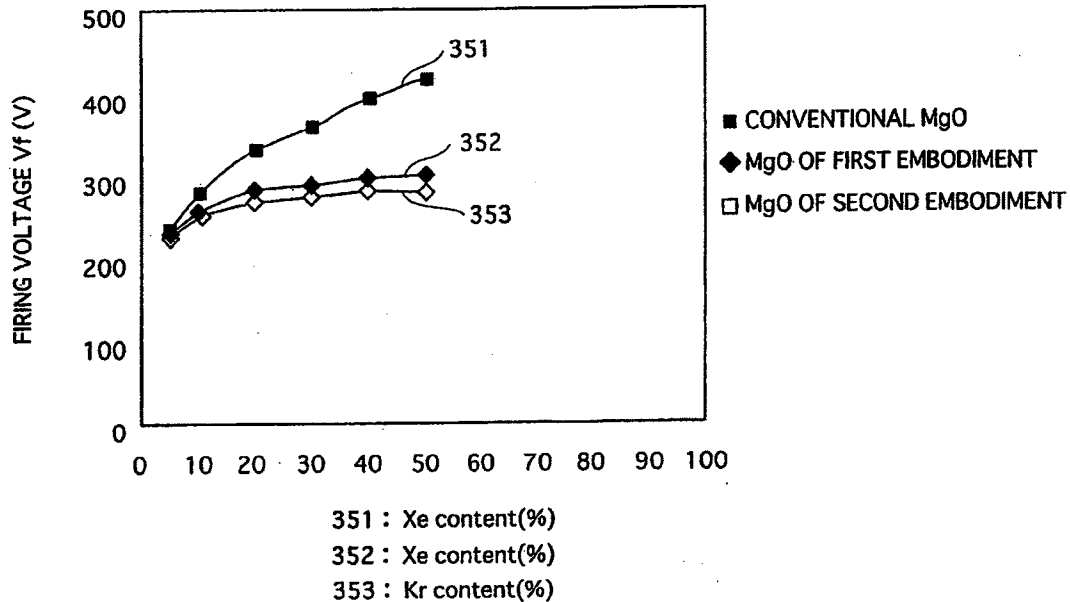
[0085] The discharge space 116 is filled with a discharge gas composed of a mixture of neon (Ne) and xenon (Xe) at a pressure of approximately 66.7 kPa (500 Torr).

[0086]   Here, the partial pressure of Xe is set to approximately 20%, which is higher than the Xe partial pressure in a discharge gas filling a standard PDP (approximately 7-10%).

The Final Office Action rejection rejected Claims 1-3 and 6 over *Kimura* (Japanese Laid-Open Application 2001-332175 under 35 U.S.C. §102.

The Office Action also rejected Claims 1-4, 6 and 13 as being anticipated by *Nakahara* (U.S. Patent No. 6,242,864).

"[A]nticipation by inherent disclosure is appropriate only when the reference discloses prior art that must *necessarily* include the unstated limitation. . . ."

Transclean Corp. v. Bridgewood Services, Inc., 290 F.3d 1364, 62 USPQ2d 1865 (Fed. Cir. 2002)

Finally, Claims 5 and 14 were rejected over the *Kimura* reference in view of *Akiyama et al.* (Japanese Laid-Open Application 2003-272533) under 35 U.S.C. §103).

The Office Action asserted that a protective layer of MgO would have apparently a generic chemical composition and that its physical and electrical properties would be inseparable from the basic chemical definition of MgO to justify a broad interpretation of a prior art utilization of MgO as a protective layer. The Office Action did not consider that our protective layer had a physically different electrical configuration resulting from creating a particular electron band and the energy level formed within a forbidden band. Our claims specifically define a particular plasma display panel with a particular partial pressure condition for the discharge gas and a specific claimed electron band having an energy level of 4 eV or less below a vacuum level formed within a forbidden band in the energy bands.

As can be readily appreciated, the claims are supported by our specification, and would be easily understood by a person of ordinary skill in this field.

More specifically, in lowering an Xe partial pressure to no less than 20%, luminous efficiency can be improved. However, the firing voltage tends to also increase which is not desirable in the large size display panels of today. This background knowledge would be understood by a person of ordinary skill, by referring to the Society Information Display 2003 (SID 2003) paper on high efficiency PDP, attached hereto.

However, in our protective layer, as defined in our current claims, an electron band including at least electrons having an energy level of 4 eV or less below a vacuum level (hereinafter, "4 eV electron band"), is specifically provided within a forbidden band in the energy bands.

Also, since a metastable state (first excited state) of Xe is originally located at energy level of 4 eV below the vacuum level, Xe ions and the protective layer easily interact with each

other. Accordingly, by performing the process of the 201a (resonance and neutralization) and the 201b (Auger neutralization) shown in Figure 2 of the present application, it is possible to efficiently emit secondary electrons from a surface of the protective film (MgO film).

FIG.2
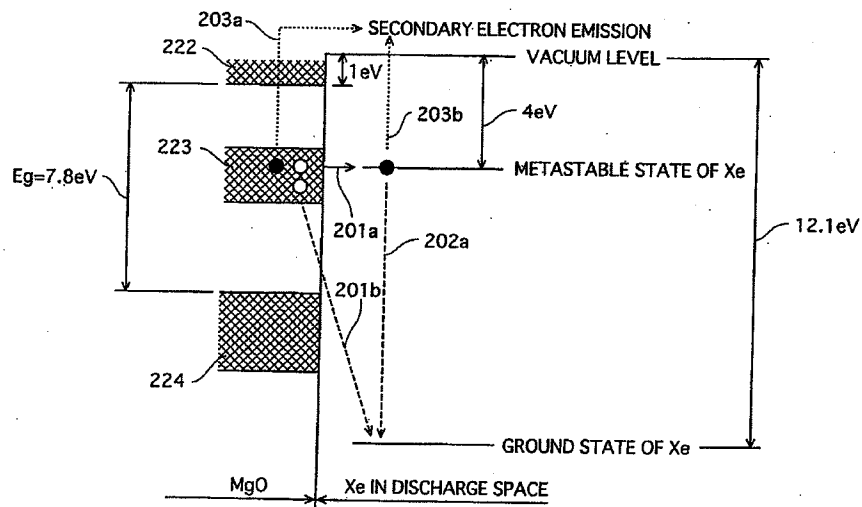
As a result, it is possible to keep the firing voltage low in the same manner as in conventional PDPs in which the Xe partial pressure is low, and still improve the luminescence efficiency.
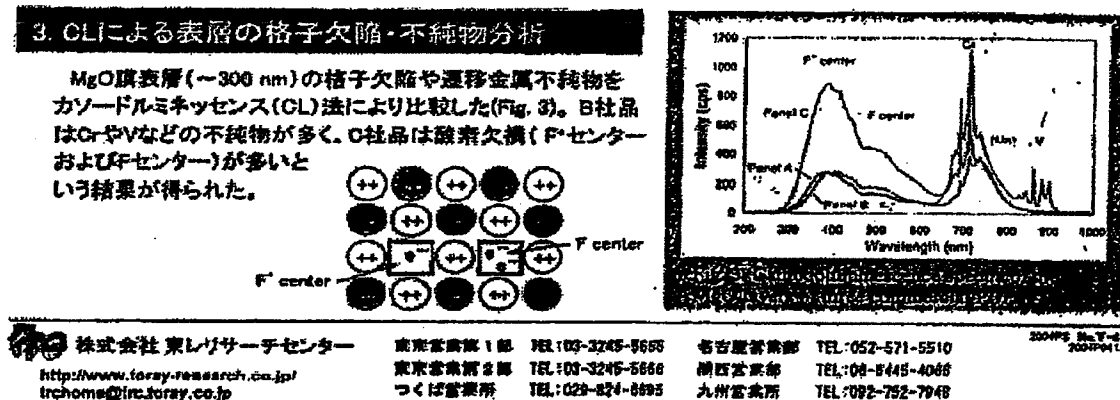
Kimura discloses technology for starting a discharge at a lower voltage by creating an oxygen deficit in magnesium oxide of the protective layer to thereby create an energy level, within a forbidden band, closer to the conduction band, and also includes a description of the protective layer having energy level, within a forbidden band, close to the conduction band. In addition, *Kimura* describes that the emission intensity is increased by injecting oxygen ions into MgO to adjust the peak wavelength of cathode luminescence to approximately 400 nm, and whereby the firing voltage can be reduced by 10%.

This adjustment of the peak wavelength of the cathode luminescence to approximately 400 nm as disclosed by *Kimura* is exactly equivalent to the characteristic 401 of a conventional protective layer described in paragraph [0123] and Figure 6 of the present application. More specifically, the characteristic 401 indicates that an emission peak of cathode luminescence is located at an energy level of approximately 3.5 eV (corresponding to a peak wavelength of approximately 400 nm).

That is, if a 4 eV electron band is formed in a protective layer, like the protective layer of the amended Claim 1 of the present application, an emission peak of cathode luminescence is located at energy level of 3 eV (corresponding to a peak wavelength of approximately 500 nm) (paragraph [0125] of the present application). Accordingly, if an emission peak of cathode luminescence is adjusted to be located at an energy level corresponding to a peak wavelength of approximately 400 nm, <u>a 4 eV electron band is not formed in the protective layer, unlike the protective layer of the amended Claim 1</u>.

As described above, the emission peak wavelength of the cathode luminescence in the amended Claim 1 significantly differs from *Kimura*. This is because the amended Claim 1 differs from *Kimura* in an electronic state of oxygen defect of a protective layer and the corresponding electrical characteristics as defined in our claims and as supported by the following technical information.

The following Figure is an excerpt from the published material attached hereto, which was disclosed in November 2004 (Toray Research Center TRC, Poster Session, 2004 Poster Cut-down Version No. V-6). This technical material describes that it is possible to specify an electronic state of oxygen defect of a protective layer with use of a measurement by a cathode luminescence method.

3. CLによる表層の格子欠陥・不純物分析

MgO膜表層（~300 nm）の格子欠陥や遷移金属不純物を
カソードルミネッセンス（CL）法により比較した（Fig. 3）。B社品
はCrやVなどの不純物が多く、C社品は酸素欠損（F+センター
およびFセンター）が多いと
いう結果が得られた。

F center

F+ center

株式会社 東レリサーチセンター

http://www.toray-research.co.jp/
trchome@trc.toray.co.jp

3.   Analysis of Lattice Defects and Impurities on Surface Layer by CL

Comparison on lattice defects and transition metal impurities on the surfaces of MgO films (up to 300 nm) is performed by Cathode Luminescence (CL) (Fig. 3). As a result, the case of the product by company S has many impurities such as Cr and V. Also, the case of the product by company C has a large amount of oxygen defect (F^+ center and F center).

According to the above material, if the emission peak wavelength is approximately 500 nm as a result of measurement by the cathode luminescence method, like the protective layer of the amended Claim 1, oxygen defect of an MgO film is mainly in a state of F center. Also, if the emission peak wavelength is approximately 400 nm as a result of measurement by the cathode luminescence method, like the protective layer of *Kimura*, oxygen defect of an MgO film is mainly in a state of F^+ center.

Here, the "F center" represents a state of oxygen defect of originally a site composed of O^{2-} to which two electrons have been trapped. Also, the "F^+ center" represents a state of oxygen defect to which only one electron has been trapped. Note that a state of oxygen defect to which no electron has been trapped (zero electron) is called "$F2^+$ center."

The state of F center, F^+ center, and F^{2+} center differ from one another in the number of trapped electrons, and accordingly, they differ from one another in energy level of an electron

band that is formed, within a forbidden band in energy bands and correspondingly in the electrical properties of MgO.

As described above, our amended Claim 1 differs from *Kimura* in an electronic state of oxygen defect in the protective layer. Accordingly, the amended Claim 1 differs from *Kimura* in the energy level of an electron band that is formed within a forbidden band in energy bands. Therefore, *Kimura* cannot exhibit the effect, unlike the amended Claim 1, that it is possible to keep the firing voltage low in the same way as in conventional PDPs even under the condition that the partial pressure of Xe is set to no less than 20%.

Nakahara discloses technology for reducing the occurrence of black noise by forming at least a surface layer of an insulating layer (arguably corresponding to the protective layer of the present application), which comes in contact with the discharge gas, with a magnesium oxide film whose impedance at 100 Hz in one square centimeter is in the range of 230-330 kΩ, or a magnesium oxide film including silicon in the range of 500-10000 weight ppm. The formation of such a magnesium oxide film increases the amount of secondary electrons emitted and makes up for a decrease in the effective voltage due to residual charge to thereby reduce the charge remaining.

However, *Nakahara* fails to recognize a problem that the firing voltage also increases under the condition that Xe partial pressure is set to no less than 20%. Accordingly, *Nakahara* neither discloses nor suggests a structure in which the energy level of an electron band that is formed within a forbidden band in energy bands of a protective layer is set to a specific energy level such that Xe ions and the protective layer easily interact with each other.

Also, the insulating layer of *Nakahara* is composed of materials including an MgO film to which oxygen defect and Si impurities have been added. However, according to the present Application, the substrate temperature for MgO film formation is in the range of 200° C to

300°C (paragraph [0119] of the present application). Compared with this, according to *Nakahara*, the substrate temperature for MgO film formation is 150°C, which is lower than the temperature in the present application. Furthermore, according to the present application, the amount of Si impurities is no more than 0.01% (100 ppm) (paragraph [0129] of the present application). Compared with this, according to *Nakahara*, the amount of Si impurities is in the range of 500 to 10000 ppm, which is greater than the amount in the present application. Therefore, the resultant final insulating layer of *Nakahara* will completely differ in physical and chemical composition from the protective layer of the present application because of conditions of the final MgO film formation.

According to the above described differences in conditions of MgO film formation, the protective layer of the amended Claim 1 and the insulating layer of *Nakahara* differ from each other in the electronic state of oxygen defect of MgO film, and accordingly, differ from each other in energy level of an electron band that is formed within a forbidden band in energy bands.

Therefore, *Nakahara* cannot exhibit an effect, as set forth in amended Claim 1, so that it is possible to maintain a discharge firing voltage at a low value in the same manner as in a conventional PDP even under our claimed condition that <u>the partial pressure of Xe is set to no less than 20%</u>.

Note, according to *Nakahara*, an emission amount of secondary electrons is increased. However, *Nakahara* uses a mechanism for increasing the emission amount of secondary electrons, which is different from our mechanism in the protective layer of our amended Claim 1.

In a standard PDP, if Xe is included in the discharge gas, the resultant Xe partial pressure in the discharge gas is low and for example 7 to 10% at most, as described in paragraph [0086] of the present application. Also, if a mixed gas such as a mixed gas of Ne and Kr and a mixed gas of Ne, Xe, and Kr is used as a discharge gas, Ne greatly contributes to the secondary electron

emission function, as described in paragraph [0052] of the present application. Accordingly, it is unnecessary to set an energy level of an electron band of a protective layer such that Xe ions and the protective layer easily interact with each other.

However, according to *Nakahara*, the emission amount of secondary electrons is increased by a setting energy level of an electron band that is formed within a forbidden band in energy bands, to an energy level where Ne and the insulating layer (protective layer) easily interact with each other.

Here, it is known to adjust energy level of an electron band that is formed within a forbidden band in energy bands in a protective layer, to predetermined energy level.

The following specifically describes forming a 4 eV electron band in a protective layer like the amended Claim 1, and then specifically describes reasons why the method disclosed by *Nakahara* cannot form a 4 eV electron band in a protective layer.

Generally, in order to form a 4eV electron band in a protective layer, the following two conditions need to be satisfied in the process of film formation of MgO (ion crystal that includes Mg^{2+} and 0^{2-}):

(A)   To secure a substrate temperature enough for again evaporating components (Mg and O) such that crystallization having a regular lattice array can be realized in the process where a flux of Mg and a flux of O to be irradiated on the substrate surface interact with each other on the substrate surface so as to be deposited as MgO; and

(B)   To appropriately adjust at least one of an introduction amount of oxygen and an amount of Mg to be irradiated on the substrate surface.

An intrinsic defect state of a formed MgO film (Mg defect and oxygen defect) is influenced by the condition (B) more strongly than by the condition (A). More specifically, in the normal film formation process, it is possible to control an intrinsic defect state of MgO by

controlling mainly the introduction amount of oxygen, and it is necessary to satisfy the above condition (A) in order to improve the controllability of the intrinsic defect state of MgO.

In a case where a state of oxygen defect is provided in an MgO film by adjusting the above condition (B), two electrons are occupied, and the state of oxygen defect transits to a state of F center in which electrical neutrality is maintained in the film because the oxygen defect in the film is a site that is originally composed of O^{2-}.

However, if the above condition (A) is not satisfied, the crystallinity of the film is insufficient. Then, a state of crystal imperfection or Mg defect is provided close to the oxygen defect, and the state of the occupied electrons transits to a state where energy level is lower. The state of oxygen defect transits to a state where plus is electronically excessive in amount, that is, a state of F^{+} center or F^{2+} center.

Furthermore, in a case where impurities are introduced, electroneutrality condition in the film is a parameter for determining an electronic state of defect or impurities, in addition to the above conditions (A) and (B).

More specifically, in a case where impurities such as Si, Ge, and Sn are included in the film, if the condition (A) is sufficiently satisfied, replacement of Mg with the impurities realizes the stability in energy. An impurity level generated as a result of this replacement is in a state where two electrons are occupied, in the same way as in an oxygen defect.

On the other hand, if the above condition (A) is not satisfied like the teaching in the case of *Nakahara*, there occurs a state where plus is electronically excessive in amount, such as the case of oxygen defect as described above. This causes a state in some center or crystal imperfection in which electrons occupied close to impurities such as Si, Ge, and Sri are taken. Also, even if an introduction amount of impurities is more than 100 ppm like *Nakahara*, crystal

distortion occurs in the same way as in the case where the condition (A) is not sufficiently satisfied, and this tends to increase its crystal imperfection.

Therefore, since the insulating layer of *Nakahara* has an introduction amount of impurities of <u>more than 100 ppm</u> and does not satisfy the condition (A), a large degree of crystal imperfection would be caused. Oxygen defect is in a state where plus is electronically excessive in amount, that is, a state in F^+ center or F^{2+} center.

Compared with this, according to the protective layer of the amended Claim 1, since the both above conditions (A) and (B) are satisfied, oxygen defect is in a state of F center, and an intrinsic defect state of Mg0 completely differs from that of *Nakahara*.

Therefore, in the protective layer of *Nakahara*, an electron band including at least electrons having energy level of 4 eV or less below a vacuum level is not formed within a forbidden band in energy bands, unlike the protective layer of the amended Claim 1. Also, *Nakahara* cannot exhibit the effect, unlike the amended Claim 1, that it is possible to keep the discharge firing voltage low in the same way as in conventional PDPs even under the condition that the partial pressure of Xe is set to no less than 20%.

As described, *Nakahara* and *Kimura* fail to recognize the problem that the firing voltage increases under the condition that the partial pressure of Xe is set to no less than 20%. Accordingly, *Nakahara* and *Kimura* fail to disclose prior art structure in which an energy level of an electron band that is formed within a forbidden band in energy bands of a protective layer is set to a specific energy level such that Xe ions and the protective layer easily interact with each other.

Therefore, even if these two references are combined with each other, would not be obvious to conceive of a structure according to the amended Claim 1 in which an energy level of an electron band that is formed within a forbidden band in energy bands of a protective layer is

set to a specific energy level such that Xe ions and the protective layer easily interact with each other. Therefore, the invention according to the amended Claim 1 involves novelty and unobviousness.

Akiyama et al. was simply cited to show Group II and VI elements in a protective layer with an additive element selected from Group IV and V having a higher concentration adjacent the discharge space to reduce a discharge start voltage. There is no teaching or suggestion to a person of ordinary skill to provide the structure of the present invention.

> "A reference may be said to teach away when a person of ordinary skill, upon reading the reference, would be discouraged from following the path set out in the reference, or would be led in a direction divergent from the path that was taken by the applicant." *In re Gurley,* 27 F.3d 551, 553 (Fed. Cir. 1994); *see KSR,* 127 S. Ct. at 1739-40 (explaining that when the prior art teaches away from a combination, that combination is more likely to be nonobvious). Additionally, a reference may teach away from a use when that use would render the result inoperable. *McGinley v. Franklin Sports, Inc.,* 262 F.3d 1339, 1354 (Fed. Cir. 2001).
>
> *In re Icon Health and Fitness, Inc.* 2007 U.S. App. Lexis 18244, *10

Furthermore, even if any other references disclose that the introduction amount of oxygen defect and the addition amount of external impurities in crystal lattice of the protective layer are adjusted, it is impossible to set an energy level of an electron band of the protective layer such that Xe ions and the protective layer easily interact with each other without the recognition of the above problem like the present Application. Therefore, the invention according to the amended Claim 1 involves novelty and unobviousness.

If the Examiner has any questions with regards to this matter, the undersigned attorney would appreciate a telephone conference.

Very truly yours,

SNELL & WILMER L.L.P.

Joseph W. Price
Registration No. 25,124
600 Anton Boulevard, Suite 1400
Costa Mesa, California 92626-7689
Telephone: (714) 427-7420
Facsimile: (714) 427-7799

Structure Evaluation of Ceramic Materials by Cathode
Luminescence and ESR

Ceramics has been utilized in various fields, for example, as
IC substrates, varistors, and capacitors for personal
computers, frequency filters for mobile phones, and magnetic
heads for hard disk drives. Ceramics is composed of crystal
particles, grain boundaries, air holes, and the like. The
performance of ceramics depends on the crystallinity of each
particle, an amount of defects and impurities of each particle,
grain boundaries, and properties of a surface of each particle.
Cathode Luminescence (CL) and Electron Spin Resonance (ESR)
are highly effective techniques for evaluating defects and
impurities included in ceramic materials.

1.   Analysis of Defect Structures and Impurities of MgO
Single Crystals by CL and ESR

1.1   Evaluation by CL

Fig. 1 shows CL spectrums of a sample A (MgO single crystals)
and a sample D (polycrystalline powders). A broad light
emission band around 400 nm observed in the sample A is
considered as a light emission band caused by F^+ center in which
one electron is trapped to oxygen defect. A broad light
emission band around 500 nm observed in the sample D is
considered as a light emission band caused by F center in which

1

two electrons are trapped to oxygen defect. Fig. 1 shows that the sample D contains a large amount of F^+ center, and both the samples A and D contain Fe, Cr, or the like in ppm order.

5   1.2   Analysis by ESR

Fig. 2 shows typical ESR spectrums of MgO samples. As a result of interaction between electron spins and nuclear spins, Mn^{2+} (I = 5/2) causes a characteristic six-line spectrum, and V^{2+} (I = 7/2) causes a characteristic eight-line spectrum. It is

10   possible to perform valence evaluation by ESR. Accordingly, it is considered that, with respect to V^{2+}, Cr^{3+}, Fe^{3+}, and Mn^{2+}, the sensitivity in evaluation by ESR is higher than that by SIMS (See List 1).

15   2.   Evaluation of Defects and Impurities of Alumina Substrate by CL

Fig. 3-1 shows an SEM image of a commercially available alumina substrate.   Fig.   3-2   shows   luminescence   intensity distribution of a luminescent line around 318 nm. Fig. 3-3

20   shows spectrums of light and dark parts shown in Fig. 3-2. According to the figures, luminescence intensity is highest around the center of each particle. Since a luminescent line around 318 nm is resulted from impurities and defects, it is considered that there are a large amount of impurities and

25   defects caused by the luminescent line around 318 nm center around the center of each particle.

2

Analysis of MgO Film for Actual Plasma Display Panel

MgO films used for protective films of front panels of Plasma Display Panels (PDPs) take an important role for determining

5 various discharge characteristics. It is necessary to optimize the quality of MgO films in order to improve the display quality of PDPs. The following provides an analysis example of MgO films for three types of commercially available plasma TVs.

10

1. Carbonate Analysis by XPS (Product by Company A)

A carbonate is sometimes formed on a surface of an MgO film, and this might exert a bad influence on the performance of a protective film. The following is an example in which an

15 amount of carbonates on a surface of an MgO film is evaluated by XPS. In case of the product by company A, an amount of carbonates is comparatively small (Fig. 1(a)).

It is important not to expose a sample to the atmosphere in order to analysis carbonates. Here, a panel is dismantled in

20 inert gas, and the dismantled panel is introduced into an analysis apparatus without being exposed to the atmosphere. For just information, a large amount of carbonates is observed in the surface of the MgO film that has been exposed to the atmosphere (Fig. 1(b)).

25

2. Analysis of Depth Profiles of Impurities by D-SIMS

Analysis of depth profiles of impurity elements contained in an MgO film is performed by Dynamic-SIMS (Fig. 2). As a result,

3

H, C, F, CI, B, Na, Al and Si are detected, in addition to Mg and O arranged in a matrix. Compared with other samples, the case of the product by company A is more likely to have high density of Na Si.

5

3.   Analysis of Lattice Defects and Impurities on Surface Layer by CL

Comparison on lattice defects and transition metal impurities on the surfaces of MgO films (up to 300 nm) is performed by
10   Cathode Luminescence (CL) (Fig. 3). As a result, the case of the product by company B has many impurities such as Cr and V. Also, the case of the product by company C has a large amount of oxygen defect (F^+ center and F center).

15

Evolved Gas Analysis of Phosphor Powders for PDP upon Heating

TPD-MS Apparatus

TPD-MS is a technique for specifying evolved gas upon heating
as a function of temperature with use of an instrument to
designed corresponding to the shape and size of each sample.
Here, the following provides a result of evolved gas analysis
by TPD-MS performed on phosphors for PDPs, which are now
starting to prevail as large and space-saving displays.

Structure of PDP

Phosphors for PDPs emit light by being excited by
vacuum-ultraviolet light generated by discharge. There is a
possibility that gas will be generated from residues included
in the phosphors due to the increase in temperature of the
phosphors upon the light emission.

Phosphor Powders

With respect to blue phosphors whose luminance deteriorates,
specific occurrence of water is observed around 250°C.

The peak temperature (Tp) of the water-occurring rate of the
blue phosphors is calculated by changing the
temperature-rising rate (ø), and an active energy ΔE is
calculated. According to this value ΔE, it is judged that
this water is obtained due to thermal decomposition.

Binder-Removing Condition and Amount of Remaining Organic

5

Materials of Phosphor Paste

A TG curve in process of binder-removing in air shows that a specific weight decrease behavior around 210°C.

5   As a result of calculating an amount of remaining organic materials by changing the binder-removing temperature and time, it proves that heat treatment temperature no more than 500°C makes the amount of remaining organic materials increase.

10

6

Evaluation of MgO Film for PDP (2)

MgO Films for PDPs are important materials that not only protect dielectric layers but also determine discharge

5   characteristics of panels. It is greatly important to properly evaluate characteristics of MgO films in order to control conditions or the like in manufacturing process. In view of this, the following provides examples of evaluations of characteristics of MgO films from various aspects.

10

1.   Evaluation of Film Structure by Cross-Sectional TEM and AFM

An MgO film is composed of columnar crystals of approximately 100 nm in diameter. Results by TEM and AFM show that the

15   columnar crystals have many spaces therebetween. Also, the size of crystals on a part of the columnar crystals closer to the surface is larger than that closer to a substrate. Furthermore, according to triangular shapes of each particle on the surface (AFM image) and an electron beam diffraction

20   image, it proves that MgO film has the (Ⅲ) orientation.

2.   Evaluation of Film Characteristics by Spectroscopic Ellipsometry

According to an evaluation result, an MgO film is not an

25   isotropic medium but has a refractive index distribution in the thickness direction of the film. The refractive index becomes higher from the interface to the surface of the film. Accordingly, the degree of crystallinity becomes higher from

7

the interface to the surface of the film. This result highly matches the above result of the observation by the cross-sectional TEM.

5   3.   Status Analysis by TG-MS and XPS

MgO films are deliquescent. Accordingly, if MgO films are left in the atmosphere, the biochemical status thereof varies. Therefore, a measure is taken in the manufacturing process of PDPs in order to activate MgO films (evacuation bake or the

10   like). In order to confirm the validity and effects of this measure, it is essential to perform status analysis of MgO films. Here, MgO films left in the atmosphere are evaluated. As a result, it proves that carbonates are formed on MgO films.

8

Structure Evaluation of Ceramic Materials by Cathode Luminescence and ESR

Fig. 1 CL spectrums of Samples A and D

A

F+

F

D

500   1000
WAVELENGTH (nm)

Fig. 2 ESR spectrum of MgO

INTENSITY (arb.units)

C   Mn^{2+}(I=5/2)

D   V^{2+}(I=7/2)

Cr^{3+}(I=0)

300   320   340   360   380
MAGNETIC FIELD (mT)
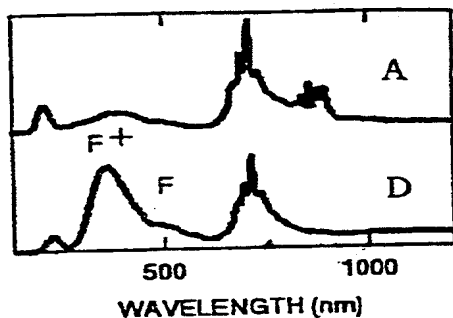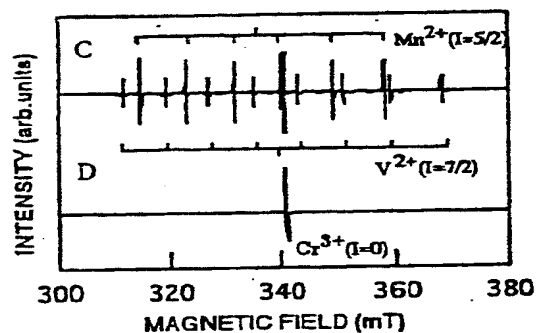
List 1 impurities of MgO

(no less than several tens ppm)

Sample	ESR	SIMS
A	Mn^{2+}(1ppm), Cr^{3+}(15ppm)	Fe, Al, F
B	Fe^{3+}(100ppm)	K, Na, Ca, Si, Ba, Ti, Al, B, Sb, Li, F, Cl
C	Mn^{2+}(5ppm), Cr^{3+}(10ppm), V^{2+}(5ppm)	Fe, Al, Mn
D	Cr^{3+}(1ppm).	—

A, B, and C : Single Crystal
D : Powder

Fig. 3-1 SEM image of alumina substrate

Fig. 3-2 luminescence intensity distribution (318 nm)

Fig. 3-3 spectrums of light and dark parts
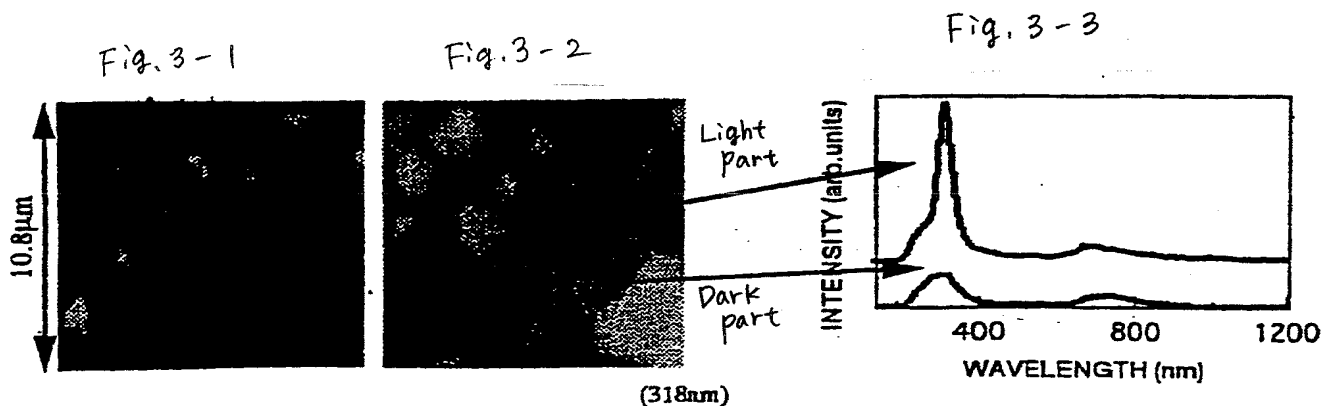
Fig. 3-1

Fig. 3-2

Fig. 3-3

10.8µm

Light part

Dark part

(318nm)

INTENSITY (arb.units)

400   800   1200
WAVELENGTH (nm)
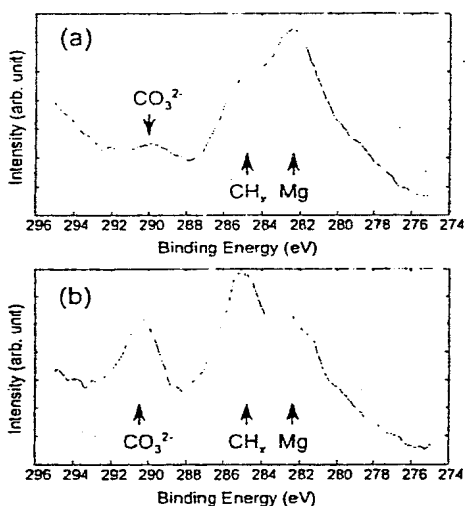
Fig. 1. Surface carbonation analysis by XPS:
(a) sampled in inert gas, and (b) after exposed
to air.
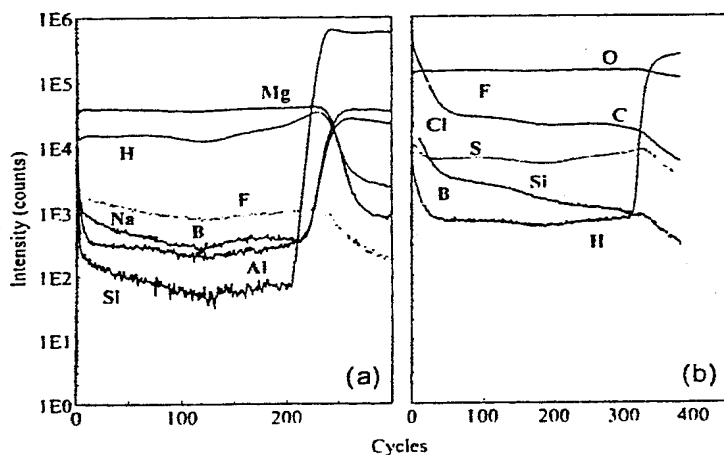
Fig. 2. Depth profiles by dynamic SIMS: (a) positive, and (b) negative
secondary ions.
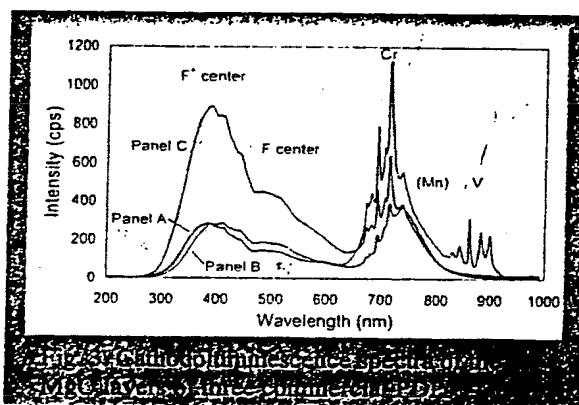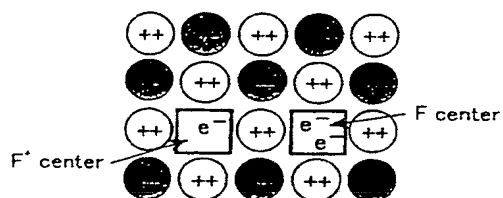
Fig. 3

Evolved Gas Analysis of Phosphor Powders for PDP upon Heating
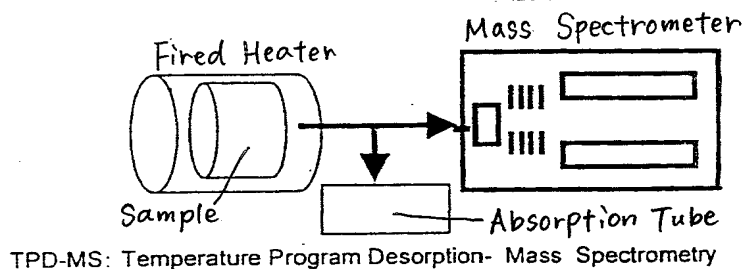
TPD-MS Apparatus

Fired Heater

Mass Spectrometer

Sample

Absorption Tube
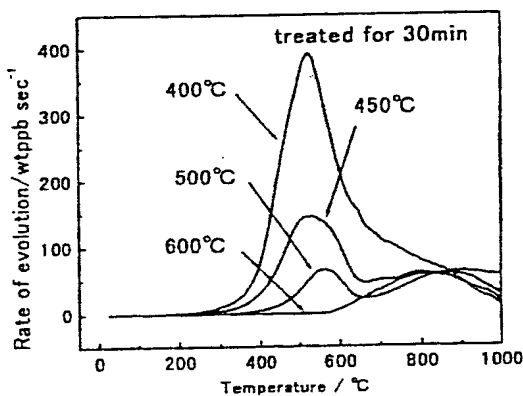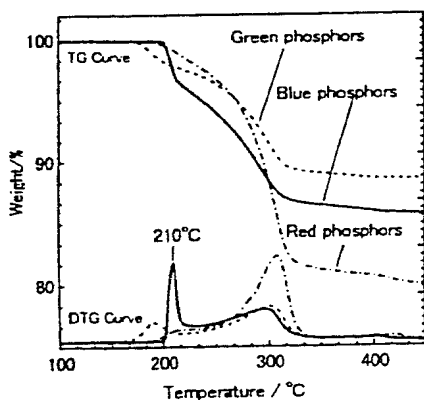
TPD-MS: Temperature Program Desorption- Mass Spectrometry

Structure of PDP

Front Panel

MgO Film

Discharge

Ne-Xe

Back Panel

Phosphor

Barrier

Dielectric

Phosphor Powders

Rate of evolution/ppm sec^{-1}

T_p

Blue phosphors (1200ppm)

Red phosphors (400ppm)

Green phosphors (20ppm)

Temperature/°C

$\log(\phi / T_p^2) = -5606/T_p + 6.77$

$\Delta E = 107.2 KJ/mol$

$\log(\Phi / T_p^2)$

$1000/T_p$
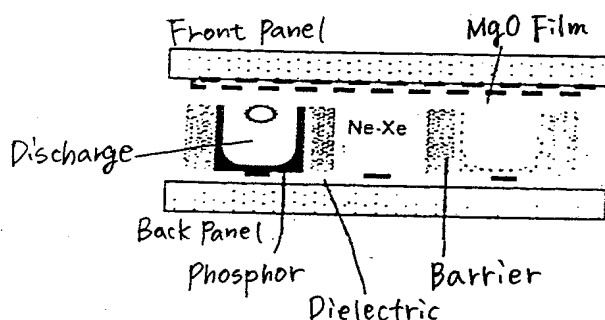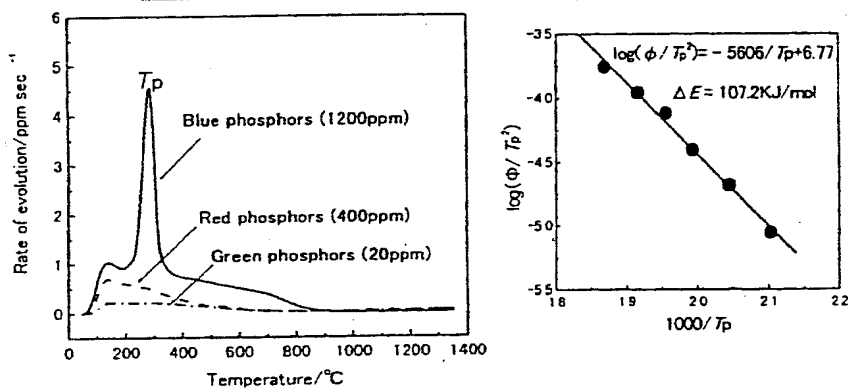
Binder-Removing Condition and Amount of Remaining Organic Materials of Phosphor Paste

TG Curve

Green phosphors

Blue phosphors

210°C

Red phosphors

DTG Curve

Weight/%

Temperature / °C

Rate of evolution/wtppb sec^{-1}

treated for 30min

400°C

450°C

500°C

600°C

Temperature / °C

Amount of CO_2 /wtppm

treated for 30min

Temperature / °C
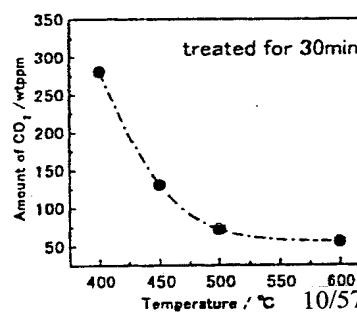
Evaluation of MgO Film for PDP (2)

1.   Evaluation of Film Structure by Cross-Sectional TEM and AFM
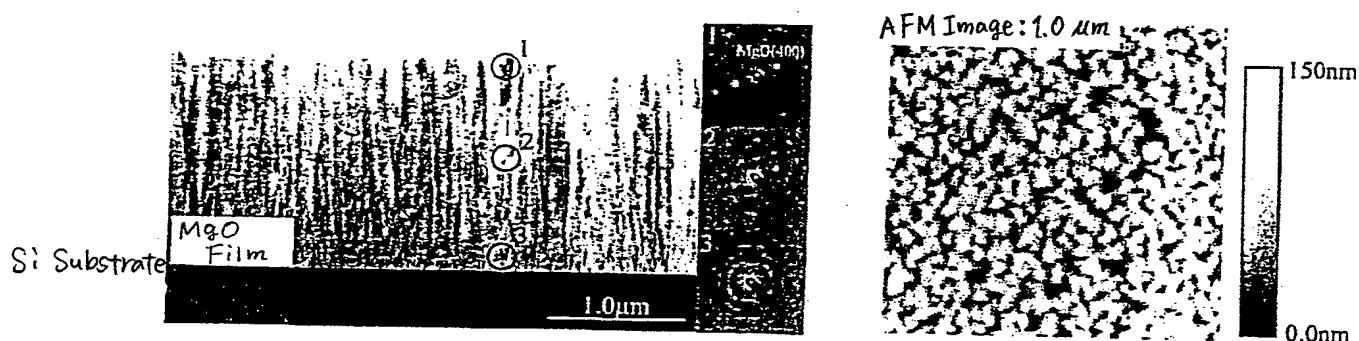
2.   Evaluation of Film Characteristics by Spectroscopic Ellipsometry
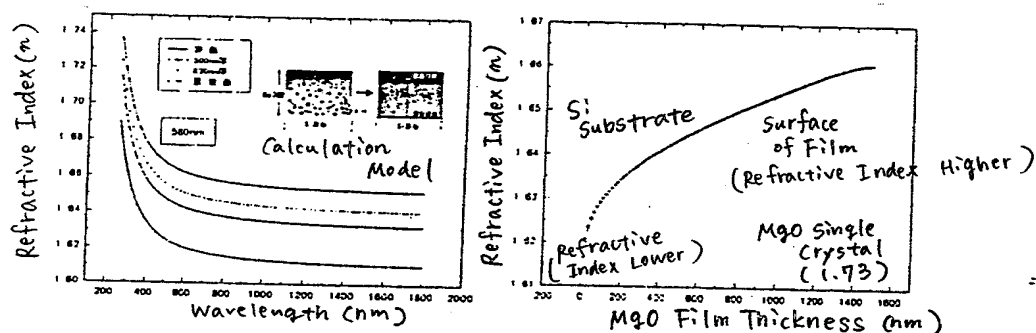
wavelength dispersion of refractive index
obtained based on calculation model

refractive index distribution
at wavelength 580 nm

3.   Status Analysis by TG-MS and XPS
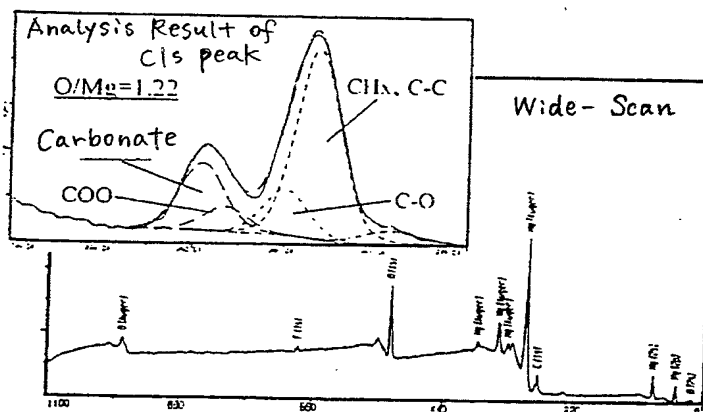
analysis result of biochemical status
of Mgo film of front panel by XPS
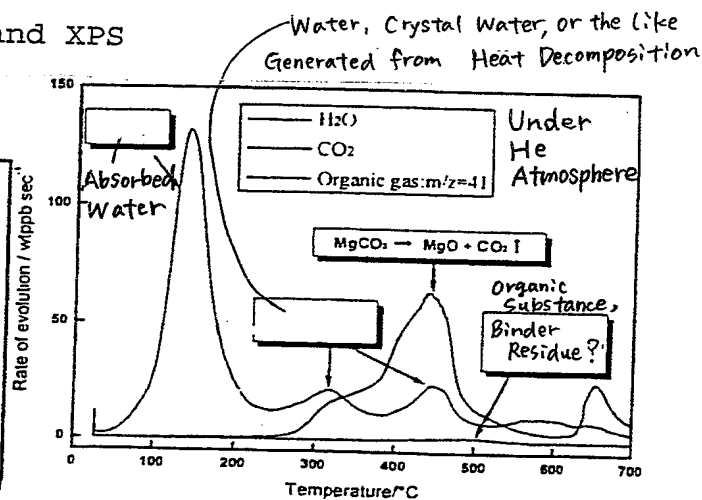
analysis result of gas generated
from front panel by TG-MS

添付資料 1

カソードルミネッセンス法及びESR法を用いた
セラミックス材料の構造評価

　セラミックスは、パソコンのIC基板・バリスタ・コンデンサ、携帯電話用の周波数フィルター、ハードディスクの磁気ヘッド等、幅広い分野で利用されている。セラミックスは、結晶粒子、粒界、気孔等から構成されており、各粒子の結晶性の度合いや欠陥・不純物量、粒界や表面の性質がセラミックス自体の性能を決定している。カソードルミネッセンス（CL）法と電子スピン共鳴（ESR）法は、セラミックス材料中に含まれる欠陥や不純物の評価を行う上で非常に有効な分析手法である。

１．ＣＬ法とＥＳＲ法によるＭｇＯ単結晶の欠陥構造と不純物分析

１．１　ＣＬ法による評価

　試料A（MgO単結晶）と試料D（多結晶粉末）のCLスペクトルを図1に示す。400nmと500nm付近に観測されているブロードな発光バンドは、酸素欠損に、それぞれ、電子が1個と2個捕獲されたF^+センターとFセンターによる発光バンドと考えられている。図1から、試料D中にはF^+センターが多く含まれており、両試料ともに、ppmオーダーのFeやCr等が含まれていることが考えられる。
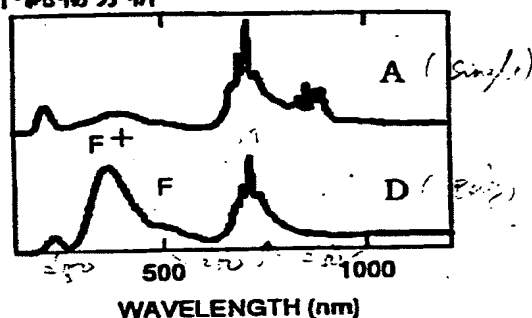
図1　試料Aと試料DのCLスペクトル

１．２　ＥＳＲ法による分析

　図2にMgO試料の代表的なESRスペクトルを示す。電子スピンと核スピンとの相互作用により、$Mn^{2+}(I=5/2)$は6本線、$V^{2+}(I=7/2)$は8本線の特徴的なスペクトルを与える。ESR分析では、価数の評価が可能であり、V^{2+}、Cr^{3+}、Fe^{3+}、Mn^{2+}に関してはSIMS分析よりも感度が高いと考えられる（表1）。
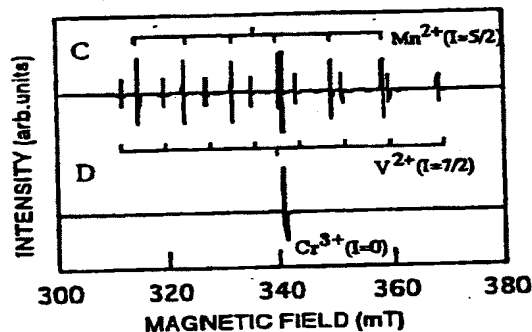
図2　MgOのＥＳＲスペクトル

表1　MgO中の不純物

試料	ESR	SIMS（数十ppm以上）
A（単結晶）	Mn^{2+}(1ppm), Cr^{3+}(15ppm)	Fe, Al, F
B（単結晶）	Fe^{3+}(100ppm)	K, Na, Ca, Si, Ba, Ti, Al, B, Sb, Li, F, Cl
C（単結晶）	Mn^{2+}(5ppm), Cr^{3+}(10ppm), V^{2+}(5ppm)	Fe, Al, Mn
D（粉末）	Cr^{3+}(1ppm)	―

２．ＣＬ法によるアルミナ基板の欠陥・不純物評価

　市販のアルミナ基板のSEM像を図3-1に示す。318nm付近の発光線の発光強度分布を図3-2に示す。図3-3には、図3-2の明暗部分を測定したスペクトルを示す。粒子の中心付近で発光強度が強くなっていることが分る。318nm付近の発光線が不純物や欠陥による発光線であることから、粒子の中心付近では318nm付近の発光線が関係した不純物や欠陥が多くなっていることが考えられる。
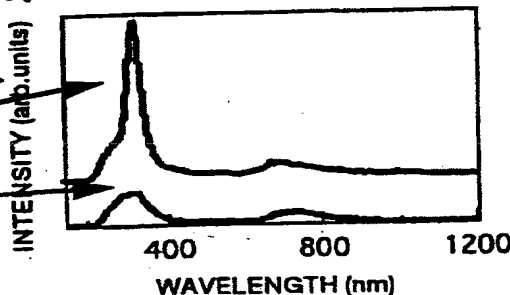
図3-1 アルミナ基板のSEM像　　図3-2 発光強度分布 (318nm)　　図3-3　明暗部分のスペクトル

株式会社　東レリサーチセンター

プラズマディスプレイ実パネルの MgO膜分析

　プラズマディスプレイ(PDP)前面板の保護膜に用いられるMgO膜は、放電諸特性を左右する重要な役割を担っている。PDPの表示品質向上のために、MgO膜の膜質の最適化が望まれる。ここでは、市販プラズマテレビ3種のMgO膜を分析した例を紹介する。

1. XPSによる炭酸塩分析（A社品）

　MgO膜表面は、しばしば炭酸塩を形成しており、これが保護膜の性能に悪影響を及ぼすことがある。表面の炭酸塩量をXPSによって評価した例を紹介する。A社品は、炭酸塩が比較的少なかった(Fig. 1 (a))。

　炭酸塩を分析する際には、試料を大気に触れさせないことが重要である。ここでは、パネルを不活性ガス中で解体し、大気に曝すことなく分析装置に導入した。参考までに大気曝露後の表面を測定したところ、多量の炭酸塩が認められた(Fig. 1(b))。
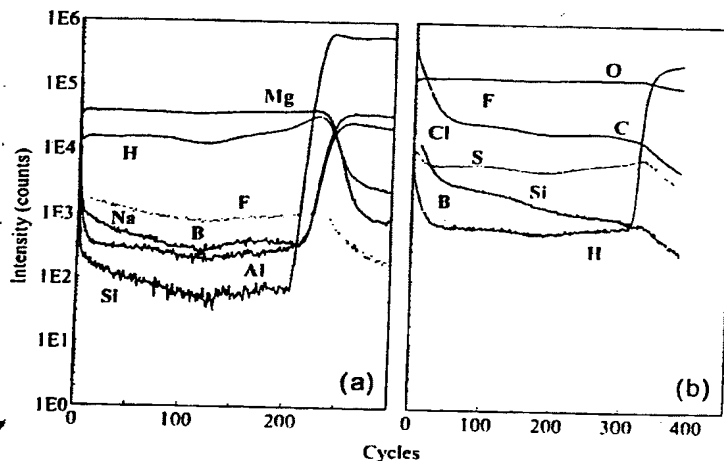
2. D-SIMSによる不純物深さ方向分析（A社品）
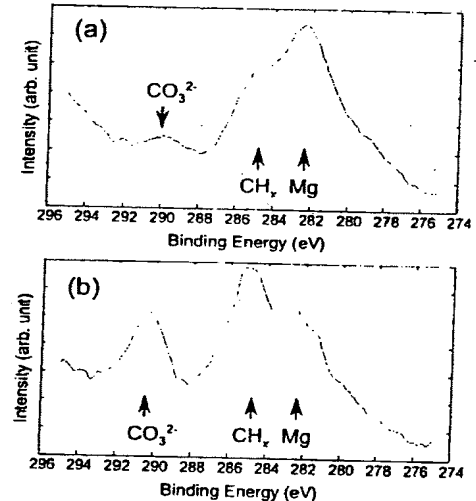

Fig. 2. Depth profiles by dynamic SIMS: (a) positive, and (b) negative secondary ions.

Fig. 1. Surface carbonation analysis by XPS: (a) sampled in inert gas, and (b) after exposed to air.

　膜中の不純物元素の深さ方向分析をダイナミックSIMSによって行なった(Fig. 2)。マトリックスのMg, O以外に、H, C, F, Cl, B, Na, Al, Si などが検出された。A社品は、他の試料に比べNa, Si濃度が高い傾向にあった。

3. CLによる表層の格子欠陥・不純物分析

　MgO膜表層（～300 nm)の格子欠陥や遷移金属不純物をカソードルミネッセンス(CL)法により比較した(Fig. 3)。B社品はCrやVなどの不純物が多く、C社品は酸素欠損（F^+センターおよびFセンター)が多いという結果が得られた。
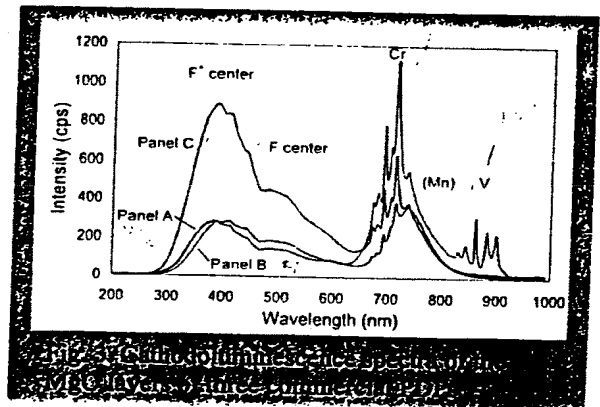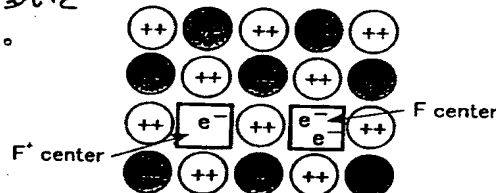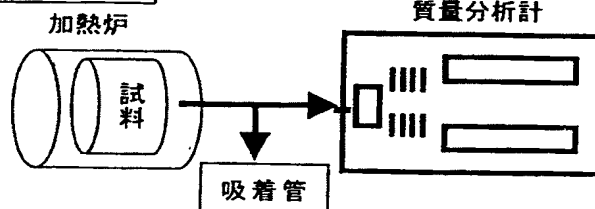
PDP用蛍光体粉末の加熱時発生気体分析

TPD-MS法とは，試料形状や試料サイズに合わせた特殊専用治具を用いて，加熱時の発生気体を温度の関数として追跡する手法である．

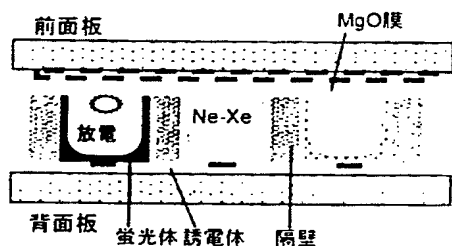ここでは，大型・省スペースのディスプレイとして普及し始めているPDPの蛍光体について，TPD-MS法を適用して発生気体分析を行った結果を示す．
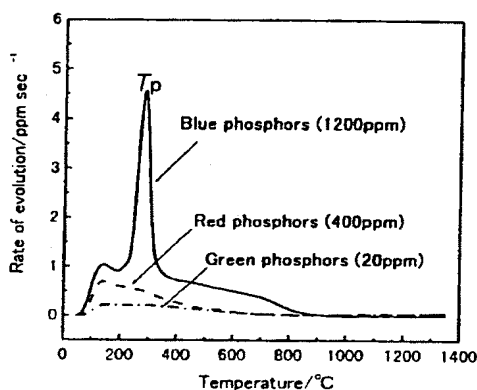
TPD-MS装置

加熱炉　　試料　　質量分析計

吸着管

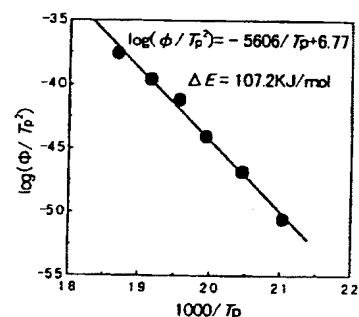TPD-MS: Temperature Program Desorption- Mass Spectrometry

PDPの構成

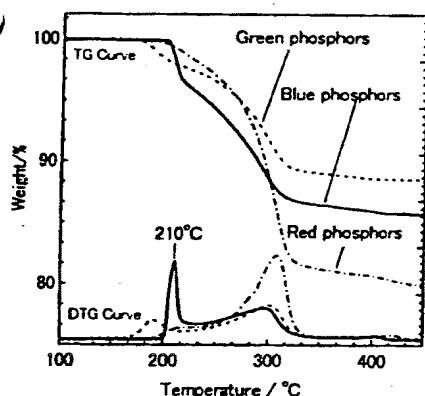PDPパネルでは，放電により発生した真空紫外光により，蛍光体を励起させて発光させている．この時の蛍光体温度の上昇などにより蛍光体中に存在する残渣物に由来した気体が発生する可能性が考えられる．

前面板　　MgO膜
放電　Ne-Xe
背面板　蛍光体　誘電体　隔壁

蛍光体粉末

T_p
Blue phosphors (1200ppm)
Red phosphors (400ppm)
Green phosphors (20ppm)

輝度劣化が問題になっている青色蛍光体では250℃付近に特異的な水の発生が認められる．
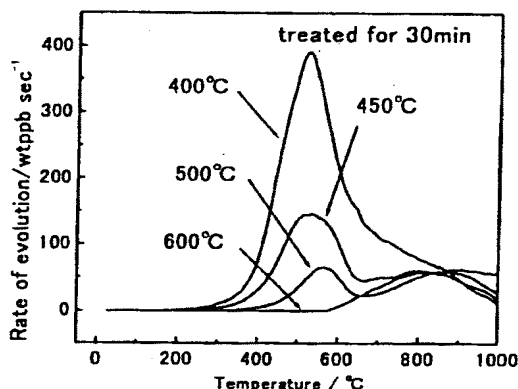

$\log(\phi/T_p^2) = -5606/T_p + 6.77$

$\Delta E = 107.2 KJ/mol$

昇温速度(ϕ)を変えて，青色蛍光体の水の発生速度のピーク温度(T_p)を求め，活性エネルギー ΔE を算出した．ΔEの値からこの水分は熱分解によるものと判断される．

蛍光体ペーストの脱バインダー条件と残存有機物量

TG Curve
Green phosphors
Blue phosphors
210℃
Red phosphors
DTG Curve

空気中で脱バインダー過程のTG曲線を測定してみると青色蛍光体ペーストで210℃付近で特異的な重量減少挙動が認められた．

treated for 30min
400℃
450℃
500℃
600℃

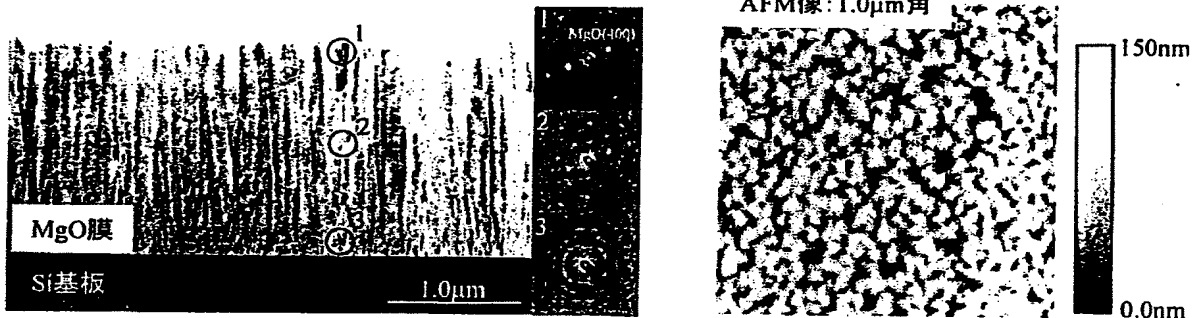treated for 30min

脱バインダー温度と時間を変えて残存有機物量を求めた結果，熱処理温度が500℃以下では残存有機物量が多くなることがわかった

TRC 株式会社　東レリサーチセンター

PDP用MgO膜の評価（２）

　PDPに用いられているMgO膜は、誘電体膜を保護するのみでなく、パネルの放電特性を左右する重要な部材である。このMgO膜の膜特性を正しく評価することは、製造プロセスにおいて条件等を制御する意味で非常に重要である。そこで、以下では様々な観点から、MgO膜の特性を評価した例を紹介する。

1. 断面TEM、AFMによる膜形態の評価

AFM像：1.0μm角

　MgO膜は、直径100nm程度の柱状結晶により形成されており、この柱状結晶の間には、空隙が数多くあることがTEM、AFM双方の結果より確認される。また、基板側に比べ、表面側では結晶子サイズが大きいことが理解される。さらに、表面の粒子形状が3角形であること（AFM像）や電子線回折像から、（111）配向を有していることが判る。

2. 分光エリプソメトリによる膜特性の評価

計算モデルより得られた屈折率の波長分散

波長580nmでの屈折率分布
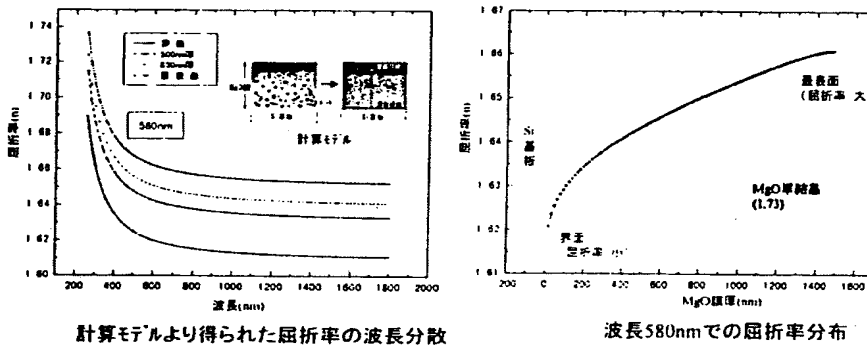
　MgO膜は、等方的な媒質ではなく、膜の厚み方向に屈折率分布が存在する膜であることがわかる。界面から膜表面に向かって屈折率が高くなっており、MgO膜の結晶性が膜表面に向かって高くなっていることがわかる。これは上記断面TEMの観察結果と良い一致をみる。

3. TG-MS法、XPS法を用いた状態解析

　MgO膜は潮解性であるため、大気中に放置すると化学状態が変化する。そのため、PDPの製造工程では、MgO膜を活性化するために処方（排気ベーク等）がとられている。この処方の妥当性、効果を確認するためにはMgO膜の状態分析が不可欠である。ここでは、大気中に放置したMgO膜の評価を行い、その結果、MgO膜は炭酸塩を形成していることが明らかとなった。
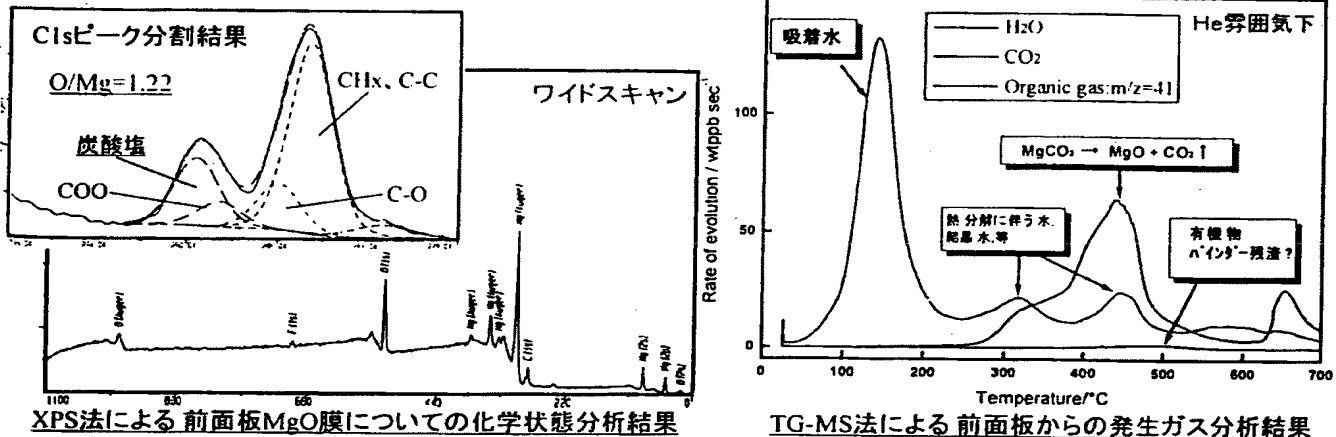
XPS法による 前面板MgO膜についての化学状態分析結果

TG-MS法による 前面板からの発生ガス分析結果

株式会社　東レリサーチセンター

2000PS No. V-4
2000P092

10/573,282
Attachment 1
Page 17 of 17

公知資料 1　(¼)

5.1: *Invited Paper:* High Efficacy PDP
G. Oversluizen, T. Dekker, M. F. Gillies, and S.T. de Zwart
Philips Research Laboratories, Eindhoven, The Netherlands

Abstract
The trade-off between PDP panel efficacy improvement and driving voltages is investigated for several design factors. It is found that for a proper combination of an increased Xe-content, cell design, and the use of a TiO_2-layer combined with "non-saturating" phosphors, a large increase of both efficacy and luminance can be realized at moderately increased drive voltages. In a 4-inch color test panel a white efficacy of 4.4 lm/W and a luminance of 5000 cd/m^2 is obtained for sustaining at 250 V in addressed conditions.

1. Introduction
The present-day PDP white light efficacy, typically about 1.5 lm/W, is rather low in comparison with a CRT (5 lm/W) and limits the brightness [1,2]. Furthermore, panel efficacy improvement implies a lower panel cost which is essential for penetrating consumer markets. Hence, efficacy improvement is a major objective in plasma display research [3,4,5].

The efficacy of an alternating current surface-discharge plasma display (PDP) can be broken down into contributions from successive conversion factors [6]: vacuum-ultraviolet (VUV) photon generation in the discharge, VUV-capture by a phosphor coating, VUV-to-visible light conversion, and visible-light losses. The discharge is a predominant factor limiting the overall efficiency. For a default PDP design with a (Ne, Xe)-gas mixture containing about 5% Xe the discharge efficiency is typically 10%[7,8]. For higher Xe partial pressure the discharge efficiency increases markedly, however, the discharge firing voltage also increases significantly [7,9,10]. Clearly, higher voltages are disadvantageous for the electronics cost. Also, for higher operation voltages a decrease of the drive margin is expected [11]. Therefore it is desired to achieve a high efficacy at the lowest attainable firing voltage.

In this paper the dependency of panel efficacy and discharge firing voltage on several cell design parameters are evaluated. Subsequently, the influence of the Xe-content in Xe-Ne gas mixtures, the dielectric layer capacitance, the sustain electrode gap and a TiO_2-layer underneath the phosphor is investigated in 4-inch, mostly monochrome test panels. Finally, the acquired knowledge is applied in a color test panel.

2. Experimental details
The design of the 4-inch test panels with 256 columns and 64 rows, which resembles the one used in main stream commercial products, has been described previously [12]. The panel luminance and efficacy is measured for continuous sustaining at 50 kHz.

Several types of test panels are used, monochrome and color, and with a default or an adapted cell design. In the monochrome green test panels, used to investigate discharge efficiency trends, a Tb-activated pentaborate phosphor is used. It was found that phosphor saturation for increasing UV-load, as reported for the Willemite phosphor [13], is no issue in this case, although the quantum efficiency is somewhat lower.

The dependence of the efficacy and firing voltage on the gas composition is investigated in monochrome test panels with default geometry. The Xe-content is varied from 3.5% to 100% at 600 hPa total pressure.

The dependence of the efficacy and firing voltage on the dielectric layer capacitance is investigated on monochrome green test panels with an Xe-concentration of 10%. In the default panel design the dielectric layer capacitance, measured on a front plate with a continuous top electrode is 0.28 nF/cm^2. In the C series this capacitance is varied from 0.15 to 0.80 nF/cm^2, and the sustain voltage is 225 V.

The dependence of the efficacy and firing voltage on the sustain electrode gap is investigated on a color panel containing a gas mixture with 13.5% Xe in Ne

The influence of a TiO_2-layer underneath the phosphors is also investigated in a color panel.

In all monochrome test panels the channels are formed by powder blasting in a glass substrate, resulting in semi-circular channel geometry.

Finally, in the color panel, used to demonstrate a high panel efficacy at a high luminance, state of the art blue and red phosphors and a dedicated green phosphor are applied. This Tb-activated triborate, $YBO_3:Tb^{3+}$, combines a high quantum efficiency and little saturation at high UV-load[11]. The powder blasting process is adapted to yield larger more U-shaped channels, which implies lower wall losses. The reflective TiO_2-layer is applied under the phosphor layer to enhance luminance and efficacy. The luminance and efficacy of the color panel is measured in addressed conditions.

3. Results and discussion
3.1 Xe partial pressure
Although the increase of the efficacy for increasing Xe-concentration, or gas pressure, is well known [7], panel data are rare. The measured dependence of the test-panel efficacy and the firing voltage on the Xe-content is shown in figure 1, for a Xe-concentration series at 600 hPa. The efficacy is normalized with respect to its lowest value and measured at a high sustain voltage of 320 V, to allow sustaining well above the minimum sustain voltage at high Xe-concentration.

Present-day commercial panels apply a Xe-concentration of 4 to 5 % at a pressure of about 600 hPa. A significant improvement thus appears conceivable. The present results are in good agreement with previous work, where we explored Xe-concentrations up to 20%, and used a numerical model to obtain

10/573,282
Attachment 2
Page 1 of 4

an estimate of the contributing factors. It was found that an increase of both the Xe-excitation efficiency and the e-heating efficiency each contribute about equally to the overall increase of the plasma efficiency [14].
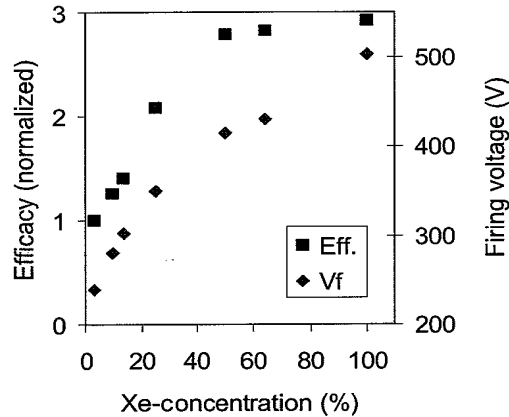

FIG.1 Dependence of the efficacy, normalized to its lowest value, and the firing voltage on the Xe concentration for continuous sustaining at 50 kHz, 320 V; the filling pressure is 600 hPa.

As expected, the efficacy increases for increasing Xe though there is a "leveling off" at a Xe content of approximately 50 %. The leveling off is anticipated. As already noted above, the typical discharge efficiency for default conditions is 10 %, which is the result of a multiplication of a 30 % electron heating efficiency and a 35 % Xe-excitation efficiency [7,8]. This limits the theoretical gain factor to 10. Naturally, ion-heating losses cannot be completely avoided since the discharge requires ionization. Also, the electron energy will be distributed, and consequently the Xe-excitation efficiency is sub-optimal for parts of the spectrum. Therefore a leveling-off at higher gain factor is expected.

Also the firing voltage increases for increasing Xe concentration. The increase of the discharge voltages is caused by the low secondary electron emission coefficient of Xe [10]. This increase is indicated by modeling and confirmed by experimental results [7,15,16]. An increasing firing voltage implies increasing operation voltages. Although the use of a somewhat higher sustain voltage even appears beneficial for the discharge efficiency, electronics cost considerations drive towards lower operation voltages. In the next sections measures to control the firing voltage are discussed.

3.2 Dielectric layer capacitance
The dependence of the test-panel efficacy and the firing voltage on the dielectric layer thickness, for a gas mixture with a Xe-concentration of 10% at 660 hPa, is shown in figure 2. The efficacy is measured in addressed conditions at a sustain voltage of 225 V. The efficacy decreases markedly for increasing capacitance, i.e. decreasing layer thickness. A similar trend has been observed in corresponding investigations on panels containing a mixture of 3.5% Xe in Ne. The decrease of the efficacy is attributed to a decrease of the electron heating efficiency for increasing capacitance [17].

The firing voltage also decreases for increasing dielectric layer capacitance. This is due to the division of the externally applied voltage over the gas capacitance and the dielectric layer capacitance, which are connected in series. For increasing dielectric layer capacitance a larger fraction of the external voltage is applied over the gas space.
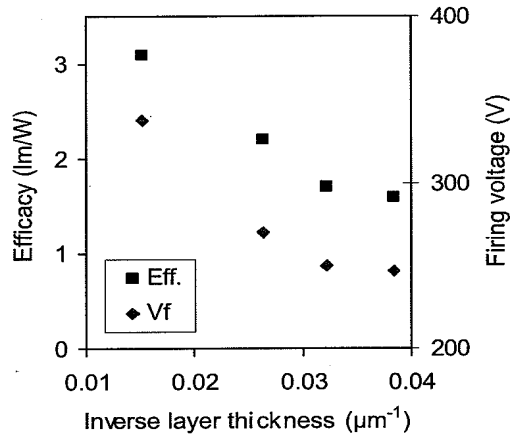

FIG.2 Dependence of the normalized luminance and the firing voltage on the dielectric layer thickness for a 10% Xe in Ne gas mixture.

It is seen that efficacy and firing voltage show a similar dependence on the dielectric layer capacitance. This implies a trade-off. A balanced design at intermediate capacitance values is required, since neither a very high firing voltage nor a very low efficacy is acceptable. Furthermore, the dynamic drive voltage margin (not discussed is this article) also shows larger values for intermediate capacitance values.

3.3 Electrode gap
The dependence of the test-panel efficacy and the firing voltage on the sustain electrode gap, for a gas mixture with a Xe-concentration of 13.5% at 800 hPa, is shown in figure 3.
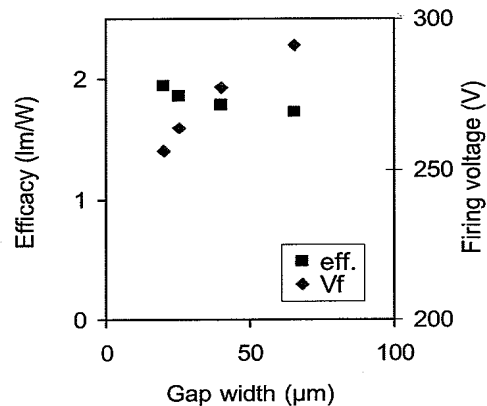

FIG.3 Dependence of the efficacy and the firing voltage on the sustain electrode gap for a 13.5%Xe in Ne gas mixture at 800 hPa.

5.1 / G. Oversluizen

The efficacy depends little on the gap width for the small gap values studied. This is expected for a surface discharge, where about 60% to 70% of the VUV radiation is generated above the cathode and 30% to 40% above the anode [18]. There is no efficient "positive column" discharge contribution, as reported for larger gap widths of 200 μm to 500 μm [19,20].

In agreement with the well-known Paschen law the firing voltage increases for increasing gap width. The minimum sustain voltage also increases, although the dependency is weaker. Therefore the static margin increases for increasing gap width. Similar results were reported previously and a corresponding trend is reproduced with model calculations [21,22].

It follows from the above that small electrode gaps are attractive, because the discharge voltages are lowered without a penalty on the efficacy. It should be noted however, that the increasing risk of dielectric breakdown also imposes a technology dependent lower limit. For common practical panel designs the gap size is governed by discharge voltage requirements, both the absolute values and the drive margins, in a regime where efficacy is not affected.

3.4 TiO$_2$-layer
In figure 4 the efficacy of color test panels with and without a TiO$_2$-layer underneath the phosphor is compared. The efficacy (triangles) is seen to increase for increasing sustain voltage with a roughly similar characteristic for both panels. The voltage dependence of the efficacy is affected by many factors, amongst others the Xe-content and the sustain frequency [12,23]. It is clear that, a marked increase of the efficacy, by about a factor of 1.5, is observed upon addition of a TiO$_2$-layer underneath the phosphor. For panels without such a layer the visible light emission at the backside is about 20%. Thus, recovery of this backside emission cannot fully account for the efficacy improvement, which also appears to be somewhat dependent on the sustain voltage. Apparently the discharge efficiency increases.
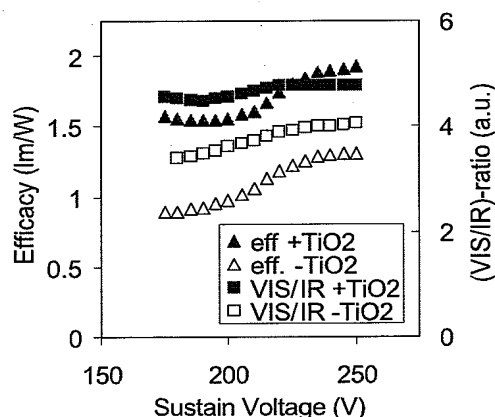

FIG.4 Comparison of the efficacy and the (VIS/IR)-emission ratio for color test panels with and without a TiO$_2$-layer underneath the phosphor.

An indication for an increased Xe-excitation efficiency can be derived from the panel emission [14]. A typical spectrum contains emission in the visible region (VIS) from the phosphors, and Xe-emission with lines at 823 nm and at 828 nm in the near infrared (IR), is also prominent. The 828 nm line is due to relaxation from a higher excited Xe-state to the level Xe(^{3}P$_1$), the source of the resonant 147 nm emission, and the 823 nm line is due to relaxation from a higher excited Xe-state to the Xe(^{3}P$_2$) metastable level, a precursor for Xe-dimer radiation at 173 nm.

Xe is excited in higher Xe*-levels as well as directly into the Xe(^{3}P$_1$) and Xe(^{3}P$_2$) metastable levels. Direct excitation in these levels involves less relaxation losses and no 823 nm or 828 nm emissions. Finally, both resonant and dimer radiation excite the phosphor with a comparable efficiency and the visible emission intensity can be taken as a measure for the total VUV-intensity. Thus an increase of the intensity ratio of (VIS/IR)-radiation suggests a larger fraction of direct excitation into the lower Xe(^{3}P$_1$) and Xe(^{3}P$_2$), i.e. an increase of the Xe-excitation efficiency.

Therefore, the increase of the (VIS/IR)-ratio for a panel with a TiO$_2$-layer underneath the phosphor (see squares in figure 4) implies an increase of the Xe-excitation efficiency. The roughly corresponding voltage dependence of the efficacy and the (VIS/IR)-ratio shows, that an increasing Xe-excitation efficiency at least partly accounts for the increase of efficacy.

Furthermore, the discharge voltages decrease when a TiO$_2$-layer underneath the phosphor is applied, as illustrated in table 1.

Table 1. Discharge voltages with/without a TiO$_2$-layer

	V$_{sm}$ (V)	V$_f$ (V)
3.5%Xe, Will., without TiO$_2$	133	217
3.5%Xe, Will., with TiO$_2$	130	210
10%Xe, color, without TiO$_2$	159	248
10%Xe, color, with TiO$_2$	152	234

Clearly, the application of a TiO$_2$-layer underneath the phosphor(s) is very beneficial for both a high discharge efficiency and a decrease of the discharge voltages.

3.5 High efficacy color panel
It follows from the above that for a proper combination of Xe-content and cell design, i.e. capacitance, electrode gap and a TiO$_2$-layer underneath the phosphor(s), efficient VUV-generation at moderate drive voltages can be achieved. This knowledge is applied in a 4-inch color test panel, where dedicated phosphors, that maintain high conversion efficiency at high VUV-load, are used [11]. Figure 5 shows the sustain voltage dependence of efficacy and luminance for two color test panels with a high Xe-content.
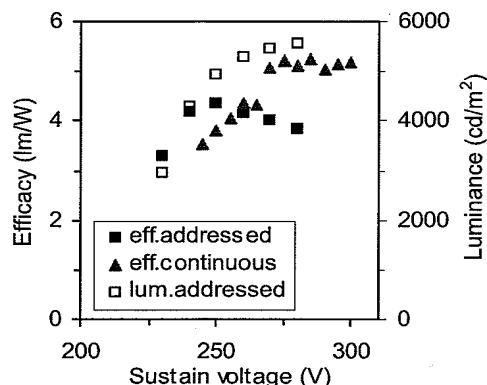
FIG.5 Efficacy and luminance as a function of sustain voltage for two high Xe partial pressure color test panels: measured in addressed conditions for a 30% Xe in Ne gas mixture (squares), and measured in continuous sustain condition for a 50% Xe in Ne mixture (triangles).

In addressed conditions, an efficacy of 4.4 lm/W and a white luminance of about 5000 cd/m^2 are concurrently obtained at a sustain voltage of 250 V for a panel containing a 30% Xe in Ne gas mixture. These values represent a large improvement in comparison with present day commercial panels, where about 1.5 lm/W and 600 cd/m^2 is usual. Moreover, in continuous sustaining condition at V>270V a panel efficacy of more than 5 lm/W has been realized in a 50% Xe-panel.

4. Conclusion

It is concluded that by proper combination of an increased Xe-content, a balanced cell design, "non-saturating" phosphors, and the use of a TiO$_2$-layer underneath the phosphor, a marked improvement of PDP efficacy and luminance can be realized, at moderately increased drive voltages. In a 4-inch color test panel a white efficacy of 4.4 lm/W and a luminance of 5000 cd/m^2 is obtained for sustaining at 225 V in addressed conditions.

References

[1] H. Bechtel et al., IDW'98, p527.
[2] K. Amemiya, T. Komaki, T. Nishio, IDW'98, p531.
[3] L.F. Weber, Euro Display'99, p1.
[4] T. Shinoda, Eurodisplay'02, p265.
[5] S. Mikoshiba, Information Display 10, 19 (2002).
[6] H. Doyeux and J. Deschamps, SID'97, p213.
[7] J. Meunier et al., J. Appl. Phys. 78, 731 (1995).
[8] M.H Klein et al., IEICE Trans. Electron.,Vol.E83-C,1602 (2000).
[9] G. Oversluizen et al., J. SID, 9, 267 (2001).
[10] M.F. Gillies and G. Oversluizen, J. Appl. Phys. 91, 6315 (2002).
[11] G. Oversluizen et al., J. SID, 10, 237 (2002).
[12] G. Oversluizen et al., J. SID, 8, 197 (2000).
[13] S. Mikoshiba et al., J. Appl. Phys. 50, 1088 (1979).
[14] G. Oversluizen et al., J. Appl. Phys. 91, 2403 (2002).
[15] G. Oversluizen et al., IDW'00, 631 (2000).
[16] T.Yoshioka et al., IDW'00, 611 (2000).
[17] G. Oversluizen et al., Appl. Phys. Lett.,77, 948 (2000).
[18] M.F. Gillies et al., IDW'01, 837 (2001).
[19] T.Akiyama and M. Ueoka, Asia Display'95, 377 (1995).
[20] J. Ouyang et al., Eurodisplay'02, p53.
[21] S. Harada et al., 4th Asia SID'97, 45 (1997).
[22] J.-P. Boeuf et al., J. Phys.IV France c4-3, 7 (1997).
[23] T. Minami et al., Eurodisplay'02, p65.